

Simulation study of the correlation (X_{max}^μ, N^μ) in view of obtaining information on primary mass of the UHECRs

Nicuser Arsene,^{1,2,*} Octavian Sima,^{1,†} Andreas Haungs,^{3,‡} and Heinigerd Rebel^{3,§}

¹*Physics Department, University of Bucharest, Bucharest-Magurele, Romania*

²*Institute of Space Science, P.O.Box MG-23, Ro 077125 Bucharest-Magurele, Romania*

³*Karlsruhe Institute of Technology, Institut für Kernphysik, Karlsruhe, Germany*

(Dated: July 13, 2016)

In this paper we study, using Monte Carlo simulations, the possibility to discriminate the mass of the Ultra High Energy Cosmic Rays (UHECRs) by combining information obtained from the maximum X_{max}^μ of the muon production rate longitudinal profile of Extensive Air Showers (EAS) and the number of muons, N^μ , which hit an array of detectors located in the horizontal plane. We investigate the sensitivity of the 2D distribution X_{max}^μ versus N^μ to the mass of the primary particle generating the air shower. To this purpose we analyze a set of CORSIKA showers induced by protons and iron nuclei at energies of 10^{19} eV and 10^{20} eV, at five angles of incidence, 0° , 37° , 48° , 55° and 60° . Using the simulations we obtain the 2D Probability Functions $Prob(X_{max}^\mu, N^\mu | p)$ and $Prob(X_{max}^\mu, N^\mu | Fe)$ which give the probability that a shower induced by a proton or iron nucleus contributes to a specific point on the plane (X_{max}^μ, N^μ) . Then we construct the probability functions $Prob(p | X_{max}^\mu, N^\mu)$ and $Prob(Fe | X_{max}^\mu, N^\mu)$ which give the probability that a certain point on the plane (X_{max}^μ, N^μ) corresponds to a shower initiated by a proton or an iron nucleus, respectively. Finally, a test of this procedure using a Bayesian approach, confirms an improved accuracy of the primary mass estimation in comparison with the results obtained using only the X_{max}^μ distributions.

PACS numbers:

I. INTRODUCTION

The mass composition of the primary UHECRs together with their energy spectrum and arrival directions are the fundamental data when searching for the sources and the acceleration mechanisms of the cosmic rays. Various detection techniques, such as surface detectors (scintillation modules [1] or water Cherenkov tanks [2]), fluorescence detectors [3], [4], radio antennas [5], microwave detection [6], have been proposed to study these observables. Despite concerted efforts in many experiments, such as Pierre Auger Observatory [7], Telescope Array [8], HiRES [9], AGASA [10] to answer these fundamental questions, a clear answer is not yet given.

In the present work we focus on the problem of the properties of the primary particle which initiates the EAS using the informations from the ground particle detectors.

One observable which is sensitive to the mass of the primary particle is the atmospheric depth where the density of the secondary charged particles reaches its maximum. This observable decreases roughly proportionally with the logarithm of the mass A of the primary particle. Its sensitivity to A is illustrated by the difference in the values for p and Fe induced showers of about 100 g cm^{-2} [11] at the same energy. It can be obtained

experimentally by measuring the shower UV light with fluorescence detectors (FD) [7], [3], [8], [9]. Indeed, the intensity of UV light emitted from an elementary volume consequent to the excitation of the nitrogen molecules in the atmosphere by the secondary charged particles in EAS, is proportional with the charge density. Thus, with the FDs the dependence of the charged particle density on atmospheric depth can be obtained. The drawback of this technique is the low duty cycle of FD measurements (up to $\sim 15\%$ [7]), due to the fact that the UV light from an EAS can be measured only during moonless nights and only in good atmospheric conditions. This fact, combined with the low statistics of the UHECRs at $E > 10^{19}$ eV, has a significant contribution to the uncertainty of mass reconstruction by FDs measurements.

To increase the observational duty cycle, the reconstruction of the primary mass on the basis of the signal of the surface detectors (duty cycle $\sim 100\%$) would be advantageous. This can be done using the reconstructed profile of the muon production depth (MPD) from EAS on the basis of the signal of the surface detectors, as proposed by Cazon et al. [12, 13] in the case of the Pierre Auger Observatory. The individual muon production depth (the muon production point expressed in units of atmospheric depth) can be calculated using the muon arrival time in the detectors and the arrival time of the shower core. Then, the longitudinal profile of the muon production rate can be obtained as the depth dependence of the number of muons produced per unit of atmospheric depth. The maximum X_{max}^μ of this profile was proposed as an observable sensitive to the primary mass.

The number of muons in the shower is also sensitive to

*nicuserarsene@spacescience.ro

†octavian.sima@partner.kit.edu

‡andreas.haungs@kit.edu

§Heinrich.Rebel@partner.kit.edu

the primary mass. However, it has a stronger dependence on the energy of the primary particle than on the primary mass, and due to this fact the uncertainty of energy determination has a high impact on mass discrimination using this observable.

In a preliminary study [14, 15] we have shown that by using the information included in the correlation X_{max}^μ versus N^μ , the accuracy of the primary mass reconstruction can be improved in comparison with the method which uses only the X_{max}^μ distribution. This correlation could also be used to test the high energy interaction models. Our preliminary study was based on simulations done with the CORSIKA code [16, 17] using the thinning option, without applying a resampling scheme. In the present work the study is extended by applying the resampling scheme proposed by Billoir [18]. Also, the parametrization of the 2D distribution X_{max}^μ versus N^μ is improved. The study is done both in the case when N^μ corresponds to all the muons from a given radial range where the muon production depth is reconstructed from the arrival times of all these muons and in the realistic case when N^μ and the production depth correspond to the muons which hit the detectors from an array like AMIGA surface detector array [19], [20], [21] of the Pierre Auger Observatory. In order to test the principle of the method, in this exploratory work the experimental uncertainties are not included and the detector simulation is not done. However, some results of the effects of uncertainties in the arrival time and in the reconstruction of the shower parameters are presented.

In Section II the observables X_{max}^μ and N^μ are introduced. In Section III the simulations used are presented and the data analysis for obtaining the muon production depth and the muon number is discussed; the resampling scheme applied is briefly described. In Section IV the 2D distribution X_{max}^μ versus N^μ is presented and parameterized. In Section V a Bayesian approach is applied in order to test the mass discrimination performance on the basis of this 2D distribution. Section VI concludes the paper.

II. THE X_{max}^μ AND N^μ OBSERVABLES

During the development of an EAS, various types of secondary particles are produced, which further interact in the atmosphere or decay. Thus, the number of secondary particles increases after the first interaction, reaching a maximum at a certain atmospheric depth, where the value depends on the mass and energy of the primary particle. The dependence of the number of charged particles on the atmospheric depth represents the longitudinal shower profile. The number of muons in the shower reaches a maximum on its development much deeper than the electromagnetic component, due to the increased production of muons when the energy of the parent pions decreases and to the larger mean free path of the muons in the atmosphere. Both the maximum of the

charged particles longitudinal profile and the maximum of the longitudinal profile of the muon production rate are sensitive to the mass of the primary particle and can also provide additional information useful to constrain the high-energy interaction models [22, 23].

X_{max}^μ can be evaluated after the reconstruction of the MPD. Experimentally the MPD can be reconstructed more accurately from the signal of the detectors from a specific radial range. This is due to the fact that the electromagnetic component of the shower can contribute to some extent to the signal of the muon detectors. Therefore, the detectors located close to the shower core, where the electromagnetic component has a much higher contribution, would introduce an uncertainty in the muon reconstruction. On the other hand, far from the shower core the number of muons decreases dramatically and also the uncertainty of the reconstruction of the MPD increases. Therefore, even if we do not simulate the detectors in our analysis we reconstruct the MPD using the muon arrival time in the observational plane (the ground plane where the detectors are located) in several radial ranges, from 1000, 1400 or 1800 m to 4000 m.

It is intuitive that for the same geometry of the shower axis, the mean number of muons on the ground will be higher for an iron induced shower compared to a proton shower of the same energy, due to the higher multiplicity at the first interactions. In fact a gross estimation of the dependence of the number of muons on primary mass and energy can be obtained using the Matthews-Heitler model [24]

$$N_t^\mu = A \left(\frac{E/A}{\xi_c} \right)^\beta, \quad (1)$$

where below the critical energy ξ_c all the charged pions are assumed to decay yielding muons, and the parameter $\beta \simeq 0.9$. As can be seen from this equation, N_t^μ has a strong, almost linear, dependence on energy whereas the dependence on mass is much weaker. Therefore, the direct use of N_t^μ for mass discrimination requires a very accurate determination of energy; also, the evaluation of N_t^μ from the signal of the detectors requires a good description of the muon lateral distribution function, i.e. a good reproduction of the experimental dependence by the theoretical functions.

In our study the muon number is obtained from simulations and N^μ represents the number of muons which hit the detectors from a specific array with an energy threshold of 300 MeV. In addition, for the purpose of comparison with an ideal situation, we consider also the case when N^μ represents the total number of muons which reach the ground in a given radial range.

III. SIMULATION DATA AND EVALUATION OF X_{max}^μ AND N^μ

A. Simulations

The statistics of this analysis is based on 120 CORSIKA simulations for each primary particle type (*proton* and *iron*), energy (10^{19} eV and 10^{20} eV) and incidence angle (0° , 37° , 48° , 55° and 60°). Thus in total 2400 simulated showers were analyzed. In the simulations the EPOS hadronic interaction model for high energies [25] and FLUKA for low energies [26] were used. The thinning level (see Section C) was set to 10^{-6} and the maximum weight to 1000. For concreteness, the simulations were done with the Earth's magnetic field corresponding to the location of the Pierre Auger Observatory and the data analysis was based on a detector array with detector separation of 750 m, similar with the AMIGA array [19].

B. Muon arrival times from EAS

The idea of using the information of the muon arrival times in order to estimate the nature of the primary UHECR was previously studied in [27–29] in the context of the KASCADE experiment [30] and later in [12, 13, 31, 32]. The principle of the method is to reconstruct the longitudinal distribution of the MPD in EAS based on the times when the shower muons reach the ground relative to the time when the shower core reaches the ground. The method is applicable to experiments which can record the temporal signal of the secondary particles at ground level, such as the Pierre Auger Observatory. One of the advantages of this method is due to the duty cycle of the surface detectors which is $\sim 100\%$, and therefore much higher than of the fluorescence detectors.

The lifetime of the muons in the EAS is quite large and the deviation in the Earth's magnetic field is very small, so one can consider that the muons travel in straight lines through the atmosphere from the production point, close to the shower axis, to the ground. Thus, if the kinematic delay [13] and the scattering effects are small, the muon production locus can be calculated using the difference between the time t_μ of arrival of muons in the detector and t_c of the shower core at ground. The basic idea is the following. Consider a shower in which the first interaction of the primary UHECR takes place in the point P (Fig. 1). A muon is produced in the point A at time t_0 (the arrival time of the core in A) and registered at time t_μ in a detector located in B . The shower core reaches the ground in point O at time t_c . The difference between the pathlengths AB of the muon and AO of the shower core is equal to $v_\mu (t_\mu - t_0) - c (t_c - t_0)$, where v_μ is the average muon speed and c is the speed of the shower front (speed of light); if the kinematic correction is negligible, v_μ is practically equal also with c .

In simulated showers the distance OB is known, as

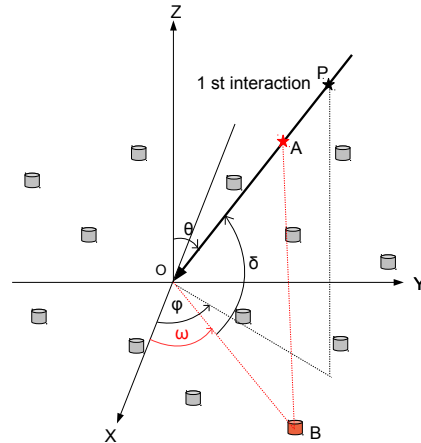


FIG. 1: Coordinate system of the EAS according with CORSIKA [15]. P = point of the first interaction, A = muon production point, O = shower core on ground, B = location of the muon detector.

well as the angles θ and ϕ of the shower axis and ω of the direction towards the detector. Then, with known values of the lengths of OB and $AB - AO$ and known angle in O , the triangle AOB can be resolved and the muon production point A can be determined. More precisely,

$$AO = c(t_c - t_0) = \frac{OB^2 - c^2(t_\mu - t_c)^2}{2[c(t_\mu - t_c) + OB \cos \delta]} \quad (2)$$

where δ is the angle between the shower axis and the direction OB .

Using this equation the atmospheric depth of the muon production can be calculated. Of course, we consider that the muon was produced on the shower core only if the properties of the triangle AOB are fulfilled (if the difference in the muon arrival time and the arrival time of the shower core is compatible with the difference in the traveled paths [14]). Note that since the MPD is reconstructed using the coordinates of the muons in the observation plane, not in the shower plane (perpendicular to the shower axis), the problems arising from the projection of the particle coordinates from observation plane to the normal plane (see [33]) are avoided.

After the reconstruction of the longitudinal muon profile, the maximum of the distribution X_{max}^μ is obtained by fitting the profile with the Gaisser-Hillas function [34].

In order to estimate the uncertainty of X_{max}^μ reconstruction due to the uncertainty of the arrival times and of the reconstruction of the position of the shower core, we analyzed a sample of 140 sets of simulated data. Each set was obtained from the same parent CORSIKA output file by applying a Gaussian spread with $\sigma_{t_\mu} = 20$ ns to each arrival time and with $\sigma_x = \sigma_y = 50$ m to the position of the shower core. The parent shower was induced by a proton at $E = 10^{19}$ eV, $\theta = 0^\circ$ and we considered

all the muons from the radial range $R = [1800 - 4000 \text{ m}]$. The standard deviation of the X_{max}^μ for this set of data was 1.9 g/cm^2 .

C. Resampling

The simulation process of the EAS is extremely time consuming and it requires a very large amount of data storage for the cascades induced at energies which exceed $\sim 10^{17} \text{ eV}$. The thinning method is implemented in the CORSIKA [17] code for reducing the computation time and the output size by replacing, in certain conditions, a bunch of secondary particles by a single representative particle with a weight equal to the sum of the weights of the replaced particles. The cost of this procedure is that large, artificial, uncertainties will be introduced. An extreme example of artificial fluctuations one can imagine when several detectors are placed in a radial range where in average actually one particle hits each detector. While in the simulation the particles have a typical weight of 100, according to simulations, only one detector from 100 detectors will be hit by a particle (with a weight of 100) and the others will have no hit. Thus, the spread from one detector to the other of the particle density reconstructed by the detectors will be much higher in the simulations than in the actual shower. In order to reduce the fluctuations associated with the strong thinning scheme, we applied for all CORSIKA simulations the "resampling" procedure proposed in [18].

The procedure consists in regenerating the particles around the detectors according to a Poisson distribution in a *sample region* around detectors. The area of this sample region (A_{sr}) depends on the distance to the shower axis and the nature of resampled particles (electrons, muons, hadrons) (for more details see [18]). In our case we have chosen a radial dimension $\sim 0.02 \times r_i$, where r_i is the distance of the detector "i" to the shower axis in the observational plane of the cascade. Instead of each particle with weight = n a number of n particles will be generated with the weights equal to 1 and the same nature, energy, arrival direction and times inside the sample region. Their positions are sampled from a 2D Gaussian distribution with $\sigma_{sr} = r_{sr}^i/2$, where r_{sr}^i is the radius of the sample region. The arrival times of the regenerated particles are then updated, including a smearing of the type $t' = t \times \exp(\sigma_t G)$ where G is a random number from a Gaussian distribution centered on 0 and variance 1, and $\sigma_t = 0.1$.

Due to the fact that a much higher number of particles represent the output of the resampling procedure, the fluctuations are much reduced.

In order to evaluate X_{max}^μ and N^μ a first code was developed to obtain a file containing the results of the resampling procedure applied to the data read from the original CORSIKA output files. Then the resampled files were processed for obtaining X_{max}^μ on the basis of arrival times and N^μ by counting the muons.

The data analysis was done with a code developed in the ROOT framework. Two analysis runs were done: in the first X_{max}^μ and N^μ were obtained by analyzing the information provided by all the muons that reach the ground in a given radial range (the *ideal* case), whereas in the second run only the information pertaining to the muons that hit the detectors located in that range was used (the *detector array* case).

IV. RESULTS: X_{max}^μ VS. N^μ SENSITIVITY TO THE PRIMARY MASS

It is obvious that at the same energy, on average a lighter particle will travel more deeply in the atmosphere before the first interaction than a heavier nucleus and therefore the induced EAS will have a larger X_{max}^μ value. Thus X_{max}^μ is a mass sensitive observable. At the same time, the multiplicity of the secondary particles from EAS at a certain energy depends on the mass of the primary particle, and thus the number of muons detected in the observational plane is another mass sensitive observable. It seems plausible that the correlated use of the information included in the maximum of the longitudinal profile of the muon production rate X_{max}^μ and in the number of muons N^μ may provide improved accuracy of the primary mass reconstruction. Specifically, showers induced by protons are expected to have a more important contribution in some regions of the 2D distribution (X_{max}^μ, N^μ), while showers induced by iron nuclei, in other regions, and thus the correlation (X_{max}^μ, N^μ) should provide better mass discrimination than each independent observable. Our aim is to test this conjecture.

For the mass reconstruction the Probability Functions $Prob(p | X_{max}^\mu, N^\mu)$ and $Prob(Fe | X_{max}^\mu, N^\mu)$ are required. These functions give the probability that a certain point from the plane (X_{max}^μ, N^μ) corresponds to a shower induced by a proton or an iron nucleus, respectively. These functions were obtained as follows.

First, the 2D distribution X_{max}^μ versus N^μ was constructed for each primary particle, energy and incidence angle using the simulations. In Figures 2 and 3 we represented this distribution obtained by analyzing all the showers with $E = 10^{20} \text{ eV}$ and different zenith angles. In Figure 2 (*ideal* case) the reconstruction of the muon production depths was done using all the muons which reach the observational plane in the radial range [1800, 4000 m], whereas in Figure 3 (*detector array* case) only the muons which hit the detectors located in the same radial range from the considered array were analyzed. In the latter case, significantly reduced information is available, because a very small percentage of the total number of muons reach the detectors, making it more complicated to distinguish between the species of the primary particle which induced the shower. In order to increase the statistics in the detector array case, each CORSIKA shower was used 10 times, by randomly distributing the shower core over the array.

Next, 1D distributions of N^μ and X_{max}^μ obtained by projecting the 2D distributions were analyzed to test whether a simple analytical parametrization could be used. In Figures 4 and 5 these distributions are displayed for showers with $E = 10^{20}$ eV and $\theta = 37^\circ, 48^\circ$, and 55° , in the detector array case. The N^μ distributions resemble Gaussian functions. Concerning the distribution of the values of X_{max}^μ , it is important to observe that the information on the MPD obtained from the detectors located in a specific radial range comes mostly from a specific range of atmospheric depths. For example, at high angles the muons generated at high atmospheric depth contribute less to the reconstruction of the distribution of the production depth. Thus the observed distribution appears truncated with respect to the true MPD distribution. This can be seen in Figure 5 for proton showers

at $\theta = 55^\circ$. The shape of X_{max}^μ can be approximated by a Gaussian distribution within the range of reconstructed values, so that the observed distribution can be described by a truncated Gaussian function. In the same case, the distribution for iron showers does not present this feature, and there are no values in the iron case beyond the cut observed in the proton distribution. Thus, in view of the final goal of identifying the primary particle on the basis of the distributions, as a first approximation, the truncation in the Gaussian functions can be neglected, because in the range beyond the cuts there are no X_{max}^μ values which could be wrongly attributed due to the truncation being neglected.

Using these results the probability density functions $Prob(X_{max}^\mu, N^\mu | p)$ and $Prob(X_{max}^\mu, N^\mu | Fe)$ were evaluated and parameterized by:

$$Prob(X_{max}^\mu, N^\mu | cr) = \frac{1}{2\pi\sigma_{X_{max}^\mu}\sigma_{N^\mu}\sqrt{1-\rho^2}} \times \exp\left[-\frac{1}{2(1-\rho^2)}\left(\left(\frac{X_{max}^\mu - \langle X_{max}^\mu \rangle}{\sigma_{X_{max}^\mu}}\right)^2 + \left(\frac{N^\mu - \langle N^\mu \rangle}{\sigma_{N^\mu}}\right)^2 - 2\rho\left(\frac{X_{max}^\mu - \langle X_{max}^\mu \rangle}{\sigma_{X_{max}^\mu}}\right)\left(\frac{N^\mu - \langle N^\mu \rangle}{\sigma_{N^\mu}}\right)\right)\right] \quad (3)$$

which is a two dimensional Gaussian function of variables X_{max}^μ and N^μ ; here cr represents the primary cosmic ray, i.e. p or Fe . We mention that in the preliminary study [15] the correlation between X_{max}^μ and N^μ was neglected in equation 3.

One can observe that the X_{max}^μ values increase when the zenith angle of the shower axis increases. The evolution of the parameters $\langle X_{max}^\mu \rangle$ and $\langle N^\mu \rangle$ obtained by fitting the 2D distributions with the function from equation 3 for different zenith angles and different

radial intervals in observational plane is shown in Figure 6. Of course, if we consider a larger radial range in the observational plane, the number of muons which contribute to the longitudinal distribution will increase and the X_{max}^μ value will be obtained with smaller uncertainty, but in view of the discussion from Section II we restricted the analysis to detectors located in defined radial ranges. The data presented in Figures 2 and 3 and analyzed further correspond to the radial range from 1800 to 4000 m.

V. BAYESIAN TEST

Using the Bayesian approach to test this procedure we need to define certain *Prior* probabilities of proton and Fe showers and then calculate the *Posterior* probabilities that a certain point from the plane (X_{max}^μ, N^μ) corresponds to a shower induced by a proton or an iron nucleus. $Prob(X_{max}^\mu, N^\mu | p)$ and $Prob(X_{max}^\mu, N^\mu | Fe)$ represent the probability to obtain the point with the coordinates X_{max}^μ and N^μ if the primary particle was a proton or an iron nucleus. The posterior probability represents the probability that a point with the coordinates

(X_{max}^μ, N^μ) is due to a shower initiated by a proton or by an iron nucleus. Supposing certain *Prior* probabilities $Prob_i(p)$ and $Prob_i(Fe)$ which represent the abundance ratio of the primary protons and iron nuclei, we can calculate the *Posterior* probabilities:

$$Prob_a(p | X_{max}^\mu, N^\mu) = K \cdot Prob(X_{max}^\mu, N^\mu | p) \cdot Prob_i(p), \quad (4)$$

$$Prob_a(Fe | X_{max}^\mu, N^\mu) = K \cdot Prob(X_{max}^\mu, N^\mu | Fe) \cdot Prob_i(Fe), \quad (5)$$

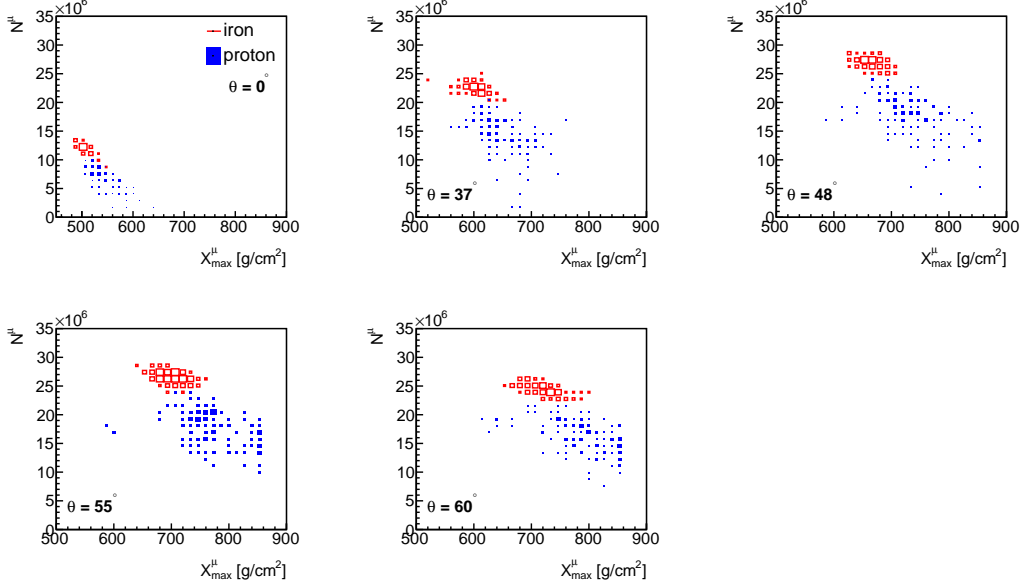


FIG. 2: Event by event analysis, number of muons at ground level in the radial range [1800 - 4000 m] versus X_{max}^μ . All the muons from this radial range were analyzed for obtaining X_{max}^μ and N^μ . 120 CORSIKA simulations per case, at $E = 10^{20}$ eV and five zenith angles.

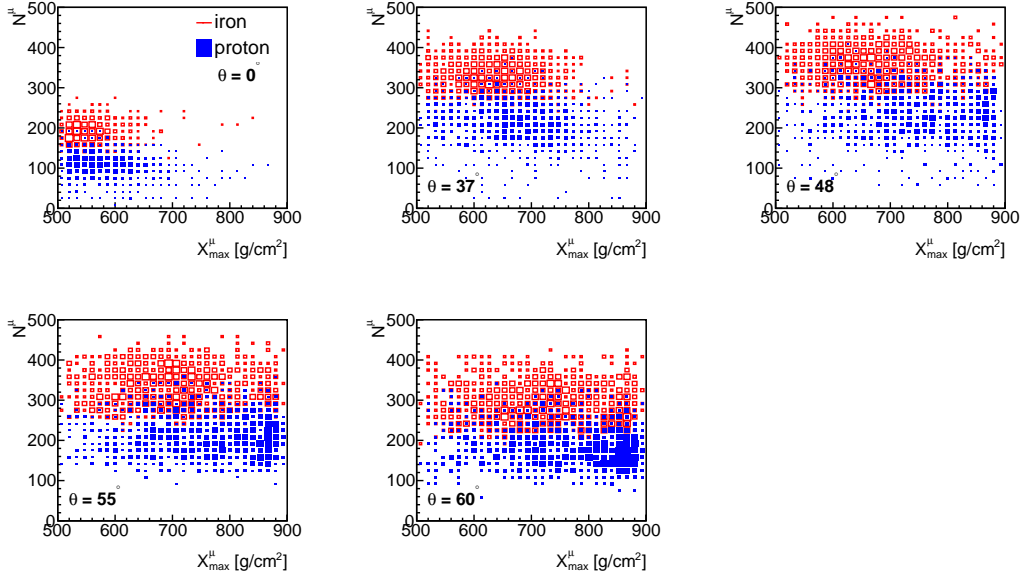


FIG. 3: Event by event analysis, number of muons at ground level in the radial range [1800 - 4000 m] versus X_{max}^μ . The information on X_{max}^μ and N^μ is obtained by analyzing the muons which hit the detectors from this radial range. 1200 CORSIKA simulations per case, at $E = 10^{20}$ eV and five zenith angles.

where the constant K can be calculated from the normalization:

$$Prob_a(p \mid X_{max}^\mu, N^\mu) + Prob_a(Fe \mid X_{max}^\mu, N^\mu) = 1. \quad (6)$$

To prove the stability of the method, we vary the prior probabilities between 0.1 to 0.9 and check the ability

of the method to reconstruct the fraction of the showers close to the true values. In other words, the posterior probability should indicate the actual fraction of the showers from different mixtures. The results of this analysis are plotted in Figure 7 for the showers with $E = 10^{20}$ eV, thinning level 10^{-6} and different zenith an-

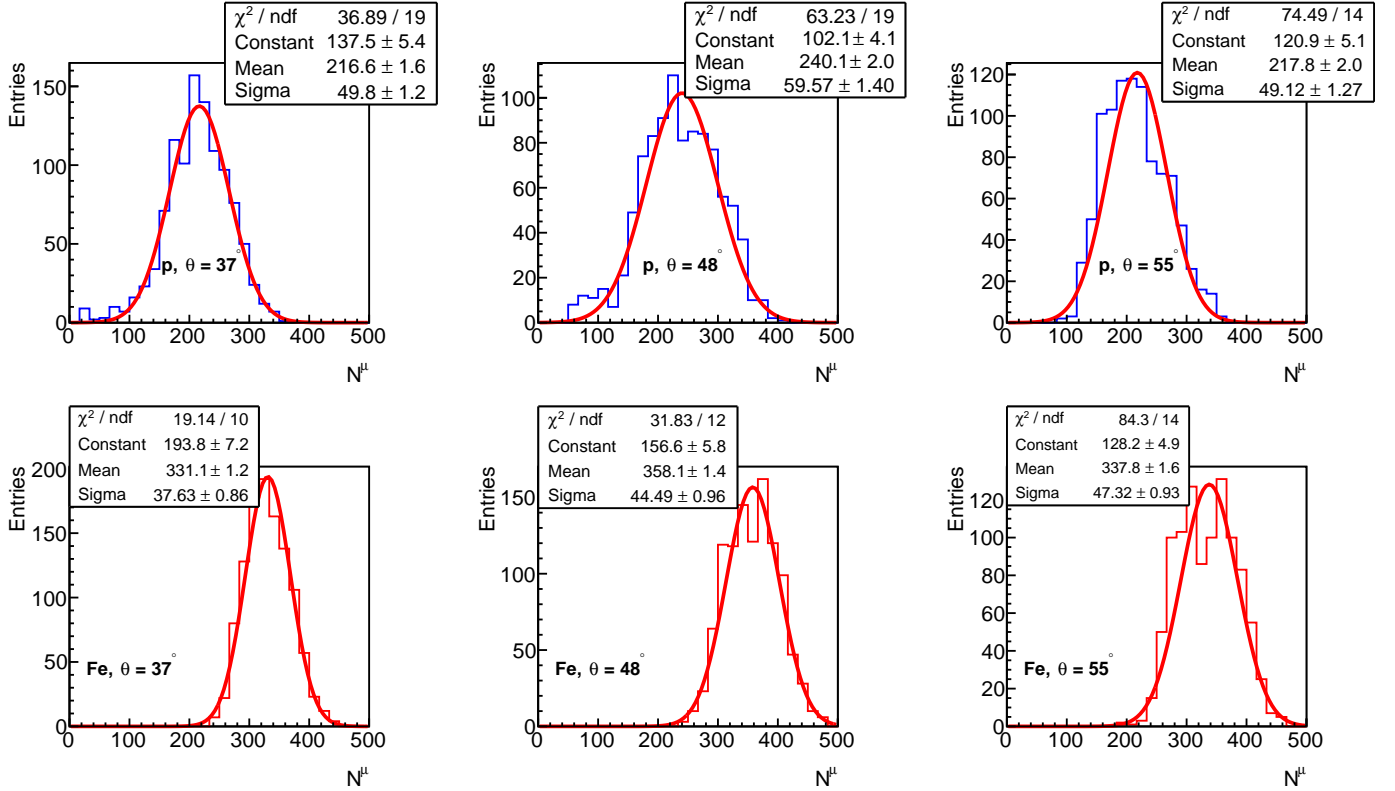


FIG. 4: Distribution of the number of muons at ground level in the radial range [1800 - 4000 m] in the detector case. Same conditions as in Figure 3.

	X_{max}^μ		$X_{max}^\mu \text{ vs. } N^\mu$	
$E[\text{eV}]$	10^{19}	10^{20}	10^{19}	10^{20}
$Prob_{p \rightarrow p}[\%]$	40	44	94	97
$Prob_{Fe \rightarrow Fe}[\%]$	52	56	96	98

TABLE I: Mass reconstruction accuracy of the methods based on X_{max}^μ and on the 2D distribution (X_{max}^μ, N^μ).

$Prob_{p \rightarrow p}$ represents the probability of correctly reconstructing the primary particle for a shower initiated by a proton (see text).

gles.

We made a direct comparison to quantify if there is an improvement in the accuracy of the primary mass reconstruction using this method of 2D Probability Function against the method which uses only the X_{max}^μ distribution. We applied these two methods for the simulations at $E = 10^{19}, 10^{20} \text{ eV}$ and $\theta = 37^\circ$. We considered a mixture of 50% proton and 50% iron induced showers and the favorable case when the correct prior probabilities are used, i.e. the prior probabilities are = 50%. We find that the reconstruction accuracy increases to $\sim 98\%$ for the method which uses the two observables (X_{max}^μ versus N^μ). The results are listed in Table I.

We emphasize that the results obtained in this analysis do not include experimental uncertainties. The un-

certainities of the values of the arrival times and of the reconstruction of the shower core position and axis angles will affect X_{max}^μ as presented in the end of Section III B. The uncertainty of the reconstructed energy of the shower will deteriorate the quality of information on mass of the primary particle embedded in the reconstructed value of N^μ ; in fact, this is the reason why the number of muons is not directly used as a mass estimator [35]. Indeed, if showers with the energy spread in a range instead of showers with fixed energy are used to construct figures similar to Figures 2 and 3, then the separation between the N^μ distributions for p and Fe induced showers will deteriorate. For example, the width of the distributions will increase from $\sigma_{N^\mu} = 1.04 \times 10^5$ to $\sigma_{N^\mu} = 4.22 \times 10^5$ for Fe induced showers if instead of $E = 10^{19} \text{ eV}$ and $\theta = 48^\circ$ the energy and the incidence angle will be distributed in the ranges $[10^{18.9}, 10^{19.1}] \text{ eV}$ and $[46^\circ, 50^\circ]$. The width of N^μ distribution for proton induced showers, which is rather large already for fixed proton energy, is practically insensitive to the relatively narrow distribution of primary energy. The difference of the average values of N^μ between proton and iron showers is practically the same in the case of fixed energy and angle as in the case of distributed values. Thus, in the presence of experimental uncertainties the mass discrimination power of the correlation (X_{max}^μ, N^μ) will be lower than that obtained in this work, but it will still remain

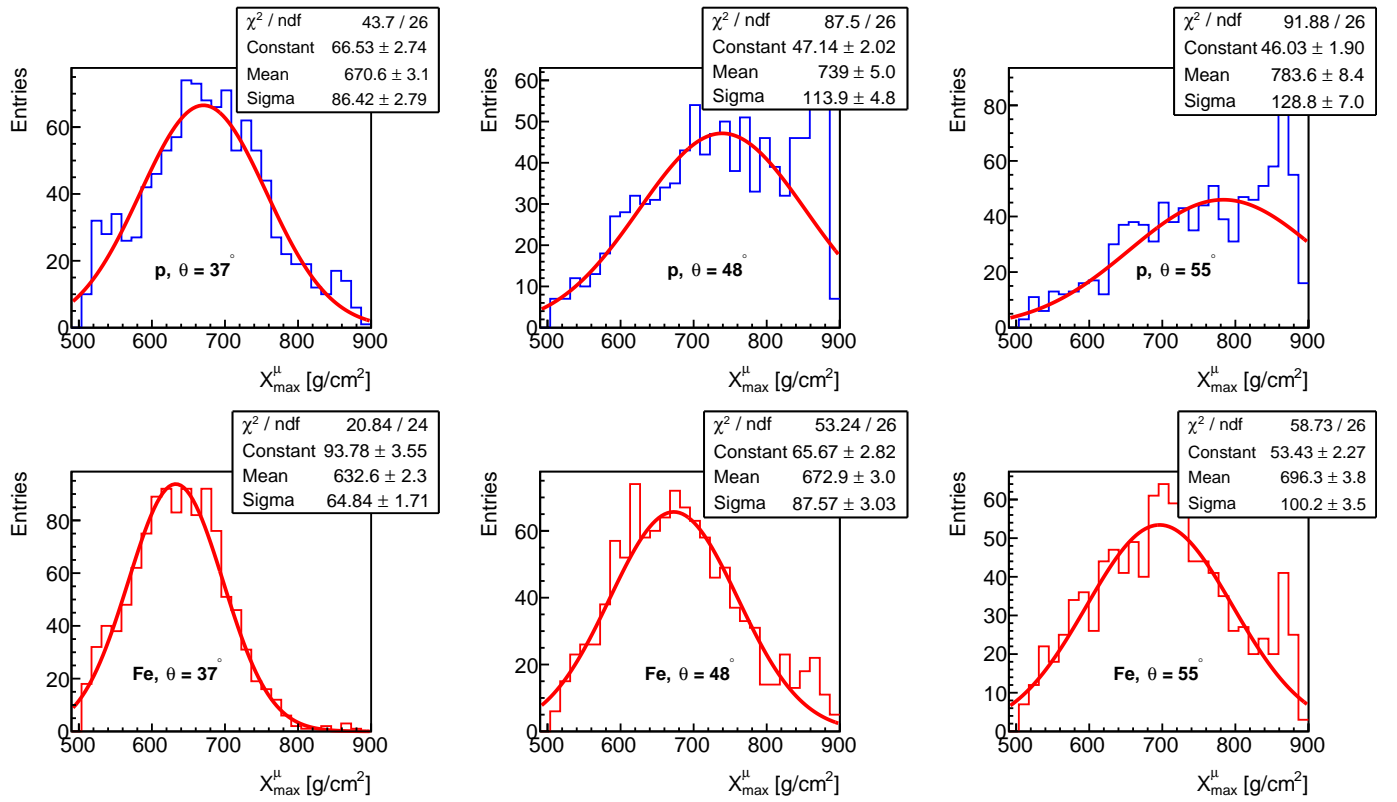


FIG. 5: Distribution of X_{\max}^{μ} obtained from the arrival time information of muons detected in the radial range [1800 - 4000 m]. Same conditions as in Figure 3.

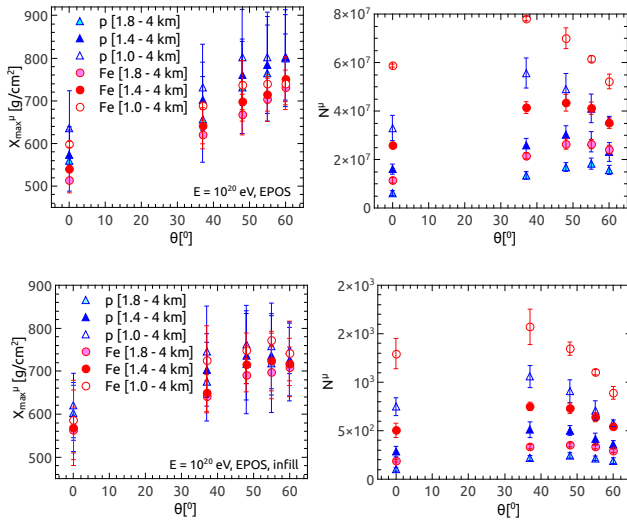


FIG. 6: The parameters obtained by fitting the 2D distributions with Eq. 3 for the showers induced at $E = 10^{20}$ eV. The plots illustrate the dependence of the parameters X_{\max}^{μ} and N^{μ} on the radial range at the ground level and the dependence on the zenith angle of the shower axis. In each case the information provided by all the muons (*top*), or only by the muons which hit the detectors (*bottom*) is used for X_{\max}^{μ} and N^{μ} evaluation.

higher than in the case when only X_{\max}^{μ} is used for mass discrimination.

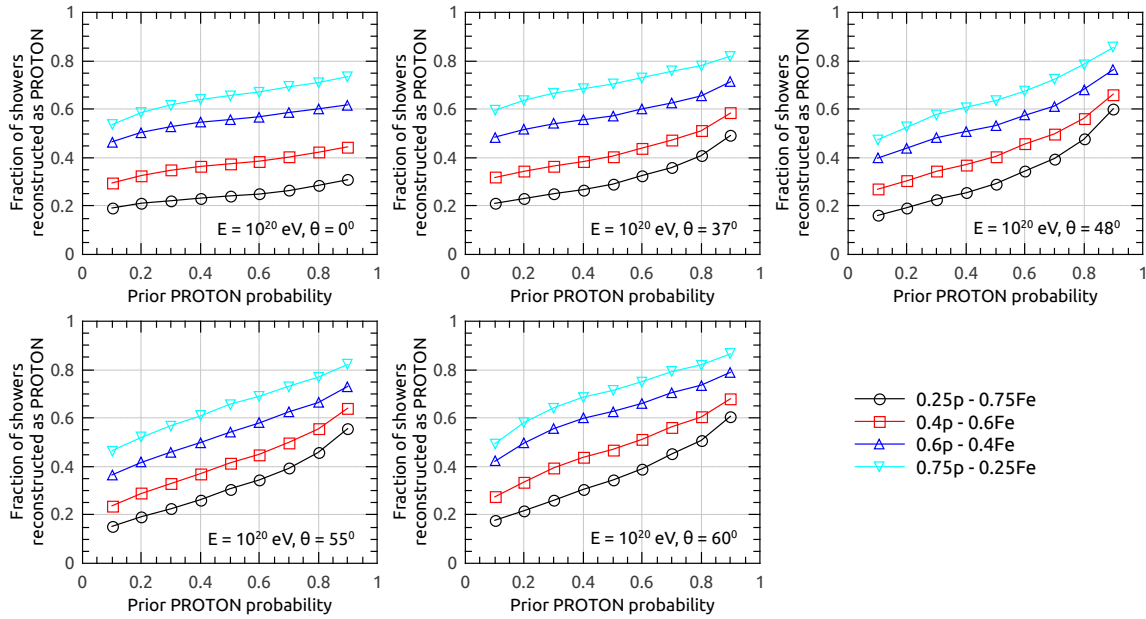


FIG. 7: Potential mass discrimination of the method. Fraction of showers reconstructed as "PROTON" for different prior probabilities, different mixtures of showers and different zenith angles at $E = 10^{20}$ eV (see text). Only the muons which hit the detectors are used for the analysis.

VI. CONCLUSIONS AND OUTLOOK

In this work, using CORSIKA simulations, we evaluated the possibility of discriminating the mass of the primary cosmic rays on the basis of the MPD taking into account the 2D distributions X_{max}^μ versus N^μ . Because both N^μ and X_{max}^μ depend on the mass of the primary particle, but in a different way, the 2D distribution may contain more information on the mass of the primary cosmic ray than the individual distributions. Using this distribution we constructed the Probability Functions $Prob(p | X_{max}^\mu, N^\mu)$ and $Prob(Fe | X_{max}^\mu, N^\mu)$ which give the probability that a certain point from the plane (X_{max}^μ, N^μ) corresponds to a proton or an iron shower.

We qualitatively found that the mass reconstruction accuracy improves when the information from the correlation X_{max}^μ versus N^μ is used in comparison with the method based only on the X_{max}^μ distribution.

Acknowledgments

The authors are grateful for the support offered by the colleagues from KIT and Pierre Auger Collaboration, especially Dr. R. Engel, D.M. J. Oehlschlaeger and Dr. D. Veberič. O. Sima acknowledges support from the Romanian Authority for Scientific Research ANCS UEFISCDI project nr. 194/2012.

-
- [1] W. D. Apel et al., *Astropart. Phys.* **47**, 54 (2013).
 - [2] M. Ave et al. (Pierre Auger Collaboration), *Nucl. Instrum. Meth.* **A578**, 180 (2007).
 - [3] J. Abraham et al., *Nucl. Instrum. Meth.* **A620**, 227 (2010).
 - [4] H. Tokuno et al., *Nucl. Instrum. Meth.* **A676**, 54 (2012).
 - [5] P. Abreu et al., *JINST* **7**, P10011 (2012).
 - [6] R. Šmída et al., *Phys. Rev. Lett.* **113**, 221101 (2014).
 - [7] The Pierre Auger Collaboration, *Nucl. Instrum. Meth.* **A798**, 172 (2015).
 - [8] T. Abu-Zayyad et al., *Nucl. Instrum. Meth.* **A689**, 87 (2012).
 - [9] P. Sokolsky, *Nuclear Physics B - Proceedings Supplements* **212–213**, 74 (2011).
 - [10] N. Chiba et al., *Nucl. Instrum. Meth.* **A311**, 338 (1992).
 - [11] *The Pierre Auger Observatory: Contributions to the 34th International Cosmic Ray Conference (ICRC 2015)* (2015), URL <http://inspirehep.net/record/1393211/files/arXiv:1509.03732.pdf>.
 - [12] L. Cazon, R. Vazquez, and E. Zas, *Astropart. Phys.* **23**, 393 (2005).
 - [13] L. Cazon, R. Vazquez, A. Watson, and E. Zas, *Astropart. Phys.* **21**, 71 (2004).
 - [14] N. Arsene, H. Rebel, and O. Sima, *AIP Conf.Proc.* **1498**, 304 (2012).
 - [15] N. Arsene and O. Sima, *AIP Conf.Proc.* **1645**, 286 (2015).
 - [16] D. Heck and J. Knapp, *Report FZKA* **6097**

- (1998), Forschungszentrum Karlsruhe; available from <http://www-ik.fzk.de/~heck/publications/> (1989).
- [17] D. Heck, J. Knapp, J. Capdevielle, G. Schatz, and T. Thouw, Report **FZKA 6019** (1998), Forschungszentrum Karlsruhe; available from http://www-ik.fzk.de/corsika/physics_description/corsika_phys.html (1998).
 - [18] P. Billoir, *Astropart. Phys.* **30**, 270 (2008).
 - [19] O. Wainberg et al., *JINST* **9**, T04003 (2014).
 - [20] M. Videla et al., *Nucl. Instrum. Meth.* **A791**, 6 (2015).
 - [21] A. Aab et al. (Pierre Auger Collaboration), Prototype muon detectors for the AMIGA component of Pierre Auger Observatory, to appear in *JINST* (2016).
 - [22] A. Aab et al. (Pierre Auger Collaboration), *Phys. Rev. D* **90**, 122006 (2014).
 - [23] P. Abreu et al. (Pierre Auger Collaboration), *Phys. Rev. Lett.* **109**, 062002 (2012).
 - [24] J. Matthews, *Astropart. Phys.* **22**, 387 (2005).
 - [25] T. Pierog, I. Karpenko, J. Katzy, E. Yatsenko, and K. Werner (2013), arXiv/1306.0121.
 - [26] A. Ferrari, P. R. Sala, A. Fass, and J. Ranft, *FLUKA: A multi-particle transport code (program version 2005)* (CERN, Geneva, 2005), URL <https://cds.cern.ch/record/898301>.
 - [27] I. Brancus et al., *J.Phys.* **G29**, 453 (2003).
 - [28] R. Haeusler, A. Badea, H. Rebel, I. Brancus, and J. Oehlschlager, *Astropart. Phys.* **17**, 421 (2002).
 - [29] H. Rebel, G. Voelker, M. Foeller, and A. Chilingarian, *J.Phys.* **G21**, 451 (1995).
 - [30] T. Antoni et al., *Nucl. Instrum. Meth.* **A513**, 490 (2003).
 - [31] S. Andringa, L. Cazon, R. Conceicao, and M. Pimenta, *Astropart. Phys.* **35**, 821 (2012).
 - [32] A. Aab et al. (Pierre Auger Collaboration), *Phys. Rev. D* **90**, 012012 (2014).
 - [33] O. Sima et al., *Nucl. Instrum. Meth.* **A638**, 147 (2011).
 - [34] T. Gaisser and A. Hillas, *Proc. of 15th ICRC 8 Plovdiv, Bulgaria* **353** (1977).
 - [35] A. Aab et al. (Pierre Auger Collaboration), *Phys. Rev. D* **91**, 032003 (2015).